Available online at www.sciencedirect.com
ScienceDirect
Scripta Materialia 63 (2010) 949–952
Scripta MATERIALIA
www.elsevier.com/locate/scriptamat

On the origin of the extremely high strength of ultrafine-grained Al alloys produced by severe plastic deformation

R.Z. Valiev,[a] N.A. Enikeev,[a,*] M.Yu. Murashkin,[a] V.U. Kazykhanov[a] and X. Sauvage[b]

[a] *Institute of Physics of Advanced Materials, Ufa State Aviation Technical University, K. Marx st., 12, 450000 Ufa, Russia*
[b] *University of Rouen, Groupe de Physique des Matériaux, CNRS (UMR 6634), Avenue de l'Université – BP 12, 76801 Saint-Etienne du Rouvray, France*

Received 2 April 2010; revised 30 June 2010; accepted 12 July 2010
Available online 16 July 2010

Ultrafine-grained Al alloys produced by high-pressure torsion are found to exhibit a very high strength, considerably exceeding the Hall–Petch predictions for ultrafine grains. This phenomenon can be attributed to the unique combination of ultrafine structure and deformation-induced segregations of solute elements along grain boundaries, which may affect the emission and mobility of intragranular dislocations.

Keywords: Ultrafine-grained materials; Al alloys; Hall–Petch relationship; Segregation

Grain refinement is well known to result in strength enhancement of metals and alloys, with the experimental relation between yield strength σ_y and mean grain size d described by the classic Hall–Petch relationship [1,2]:

$$\sigma_y = \sigma_0 + k_y d^{-1/2},$$

where $\sigma_0, k_y > 0$ are material-specific constants.

However, for nanosized grains (20–50 nm) this relation is reported to be violated so that the Hall–Petch plot deviates from linear dependence at lower stress values and its slope k_y often becomes negative. In recent years this problem has been widely analyzed in both experimental and theoretical studies [3,4].

At the same time, Hall–Petch relationship breakdown is not observed in ultrafine-grained (UFG) materials with a mean grain size of 100–1000 nm usually produced by severe plastic deformation (SPD) processing [5]. Moreover, we show in this study that UFG alloys can exhibit a considerably higher strength than the Hall–Petch relationship predicts for the range of ultrafine grains. The nature of such a markedly enhanced strength is analyzed by taking into account the grain boundary structure of UFG materials.

The objects of this research were commercial Al alloys 1570 (Al–5.7Mg–0.32Sc–0.4Mn, wt.%) and 7475 (Al–5.7Zn–2.2Mg–1.6Cu–0.25Cr, wt.%), both of which have a considerable Mg content. In order to obtain an UFG structure, solid-solute alloys were subjected to high-pressure torsion (HPT) at room temperature. HPT is known to be one of the most effective techniques for structure refinement by SPD [5]. An applied pressure of 6 GPa and 20 rotations were used to process the alloys. The produced samples had the form of discs with a diameter of 20 mm and 0.6 mm in thickness, which are well suited for mechanical tests [6].

The structural characterization was performed by transmission electron microscopy (TEM), X-ray diffraction (XRD) and atom probe tomography (APT). A mean grain size and a grain size distribution were estimated from TEM dark-field measurements in torsion plane over more than 350 grains from an area situated at the middle of an HPT disc radius. Selected-area electron diffraction (SAED) patterns have been taken from an area 1.3 μm in diameter. XRD was performed with a Pan Analytical X'Pert diffractometer using Cu K_α radiation (50 kV and 40 mA). The lattice parameter a for the initial and HPT-processed alloys was calculated according to the Nelson–Riley extrapolation method [7]. APT samples were prepared by standard electropolishing methods. Analyses were performed using a CAMECA Energy Compensated Atom Probe (ECOTAP) equipped with an ADLD detector [8]. Samples were field evaporated

* Corresponding author. Tel.: +7 347 2734449; E-mail: carabus@mail.rb.ru

1359-6462/$ - see front matter © 2010 Acta Materialia Inc. Published by Elsevier Ltd. All rights reserved.
doi:10.1016/j.scriptamat.2010.07.014

in UHV conditions with electric pulses (pulse fraction of 20%, pulse repetition rate 2 kHz). The data processing was performed using the GPM 3D Data software®. Tensile tests have been precisely performed using a laser extensometer at room temperature with a strain rate of 10^{-4} s^{-1} on a computer-controlled testing machine operating with a constant displacement of the specimen grips. Strength characteristics were estimated by testing samples with a gage of 2.0 × 1.0 × 0.4 mm.

TEM analysis proved that the HPT processing of the alloys resulted in complete refinement of the initial coarse-grained structures into UFG ones. As an example, Figure 1a,b illustrates the homogeneous UFG structure formed in the HPT 1570 alloy. A grain size distribution chart, presented in Figure 1c provides an estimate of the mean grain size of ~97 nm. The SAED pattern (Fig. 1a) exhibits typical Debye–Scherrer rings that are characteristic of ultrafine structures with mainly high-angle grain boundaries. It is also important to note that a low dislocation density inside nanoscaled grains was observed in both alloys processed by HPT (Fig. 1b), in agreement with previous studies on a Al–3%Mg alloy processed by HPT [9].

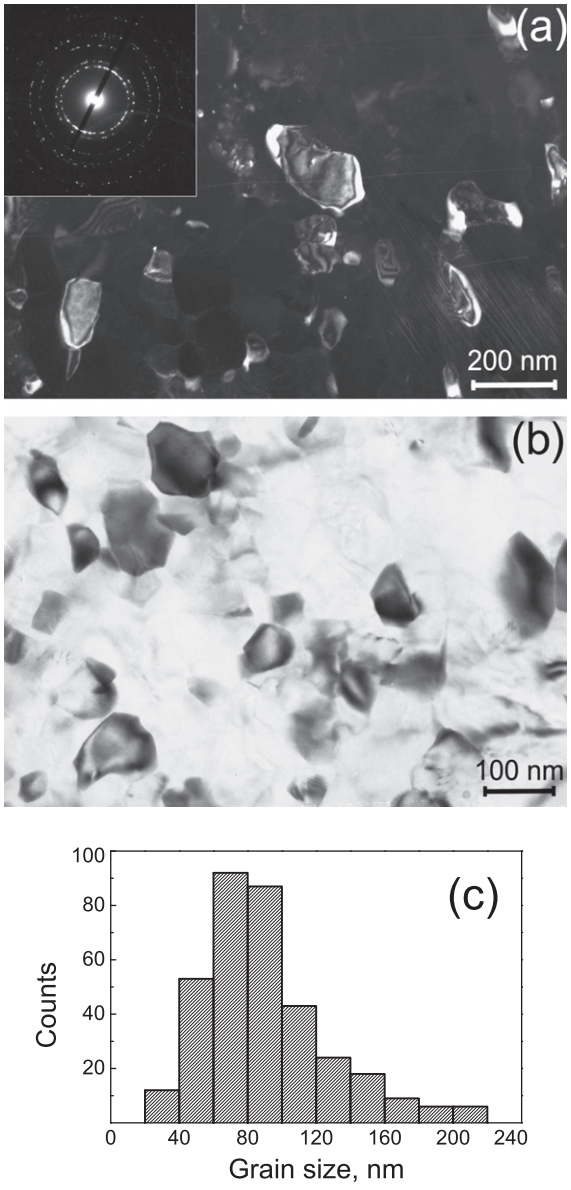

Figure 1. A typical TEM dark-field image of the UFG 1570 alloy with a corresponding SAED (a), a bright-field image (b) and a grain size distribution (c).

Figure 2 shows the results of mechanical tests of the 1570 and 7475 alloys in coarse-grained and HPT-processed states. It should be noted that deformation curves for coarse-grained states are given for 1570 alloy in the solid-solution state and for 7475 hardened by conventional T6 treatment. The plot demonstrates that UFG alloys manifest an outstanding strength accompanied by reduced uniform elongation. Both yield stress and ultimate tensile stress values exceed by almost three times those of initial solid-solution 1570 alloy, and are almost twice as much as those of T6-treated 7475 alloy.

Let us analyze the obtained data in terms of the Hall–Petch relation to estimate to what extent the exhibited strength of UFG alloys may be determined by their grain size, with special attention to 1570 alloy. There are no reference data available to construct a reliable Hall–Petch plot for the investigated alloys. In order to perform a correct comparative study we relied on the literature data for the other Al alloys.

As is known, for deformed alloys a number of factors contributes to overall hardening. For the 1570 Al alloy these include hardening caused by deformation-induced structures and solid-solution hardening. This means that the Hall–Petch slope for the materials processed by deformation techniques would be changed, as confirmed, for example, by Ref. [10] for 1100 Al alloy. The same considerations are valid for solid-solution hardening as well.

Since the investigated UFG materials have been produced by SPD, for a valid comparison we need to analyze the data obtained for Al alloys also subjected to severe straining. For that purpose two sets of data are presented (Fig. 3). The first one is for the 1100 Al alloy produced by accumulative roll-bonding [10] in order to highlight the increased k_y determined from deformation-induced structures. The second one is for UFG Al–Mg alloy produced by another SPD technique – equal-channel angular pressing [11], and shows the simultaneous effect of both deformation and solid-solution hardening. Thus, one can expect that the Hall–Petch line for Al–3%Mg alloy will demonstrate a slope typical for Al alloys, accounting for solid-solution and deformation-induced hardening.

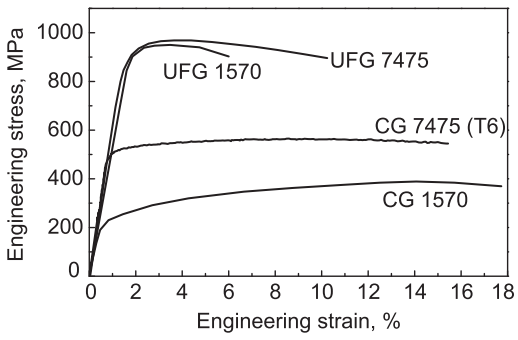

Figure 2. Engineering stress–strain curves for 1570 and 7475 alloys in UFG and coarse-grained states.

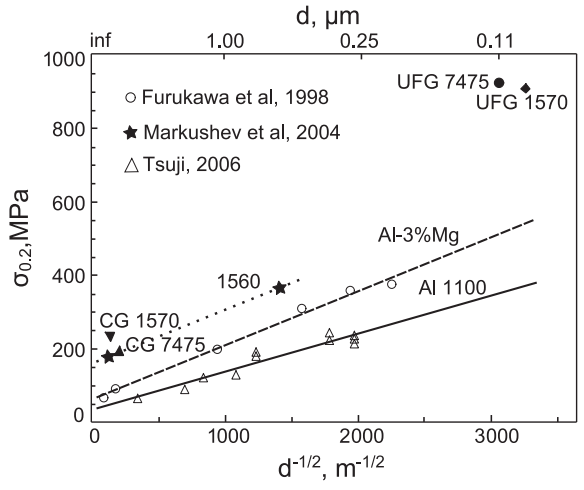

Figure 3. The Hall–Petch relation for the Al alloys: 1100 [10], Al–3%Mg [11] and data on the yield stresses of Al alloys: 1560 [12], 1570 and 7475.

Coarse-grained solid-solution-treated 1570 Al alloy had a strength value which is somewhat higher than the strength of CG Al–3%Mg alloy due to the higher content of alloying elements, the hardening contribution of which does not depend on microstructure. TEM and XRD analysis did not reveal presence of AlMg phases in UFG 1570. One could expect that the Hall–Petch slope for 1570 would not exceed that for Al–3%Mg alloy. This statement can be indirectly verified from the Hall–Petch data of a similar 1560 alloy (Al–6.0Mg–0.6Mn, wt.%) [12]. The k_y value for 1560 Hall–Petch line (Fig. 3, dotted line) is in a good agreement with the above-mentioned suggestion. However, as one can see from Figure 3, the $\sigma_{0.2}$ value for 1570 alloy is situated significantly higher than can be predicted with respect to $\sigma_{0.2}$ in the CG state. This means that the $\sigma_{0.2}$ value of 1570 alloy produced by HPT breaks down the Hall–Petch relationship for higher strengths. One can suppose that this phenomenon could not be caused only by ultrafine grain size but also by another specific features of HPT-processed alloy microstructure. Let us analyze the nature of the observed phenomena for the example of UFG 1570 alloy via detailed examination of its microstructural features.

Thanks to XRD analysis, it was determined that HPT processing significantly affects the crystal lattice parameter (a) of the Al alloys [6]. In the alloy 1570 its value is considerably reduced after processing compared to the initial state – from $a = 4.0765 \pm 0.0001$ Å to $a = 4.0692 \pm 0.0003$ Å.

The lattice parameter of Al–Mg alloys is directly linked to the amount of Mg in solid solution (1 at.% Mg resulting in a change of a by 0.0046 Å [13]). Thus, the decrease in the lattice parameter after HPT ($\Delta a = 0.0073$ Å) can be related to loss of about 1.6 at.% Mg by solid solution. Such a feature could be the result of deformation-induced segregation or precipitation at grain boundaries. APT analyses were carried out to clarify this point.

The amount of Mg in solid solution was measured in the annealed material (7.0 ± 0.2 at.%) and after HPT at room temperature (6.4 ± 0.2 at.%), confirming a decrease in the Mg content in solid solution. The discrepancy between the variations estimated from X-ray data ($\Delta c \approx 1.6$ at.%) and APT analyses ($\Delta c \approx 0.6$ at.%) might be attributed to the low statistics of APT measurements due to the small analyzed volumes. Anyway, from APT, the decrease of Mg content in solid solution could be attributed unambiguously to grain boundary segregation. As shown in Figure 4, a planar segregation of Mg was intercepted in an analyzed volume. A careful observation of the data set reveals (3 1 1) Al atomic planes on the right of the segregation, while they disappear on the left (Fig. 4b). This feature clearly indicates that there is a significant disorientation between the left and the right region separated by an excess Mg concentration along a grain boundary. Both the 2-D chemical map (Fig. 4c) and the composition profile computed across the boundary (Fig. 4d) reveal that the local concentration is up to 30 at.% Mg within a layer of about 6 nm width. It is important to note that this value is much lower than the 40 at.% expected for the Al_3Mg_2 phase, thus this Mg-rich layer along the GB cannot be attributed to the intergranular

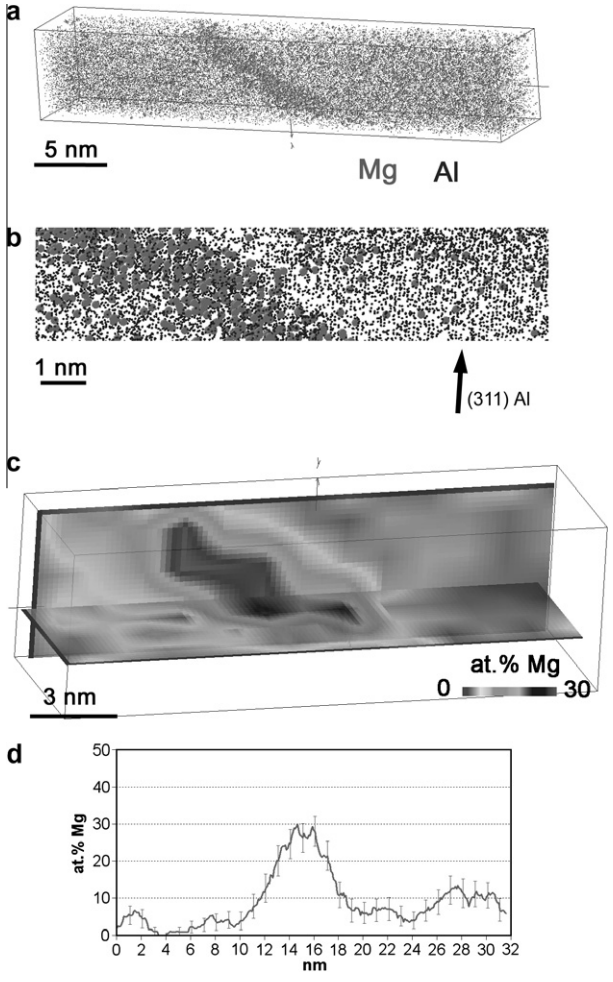

Figure 4. 3-D reconstruction of an analyzed volume in the UFG 1570 alloy: (a) full data set showing a planar segregation of Mg (Al atoms are displayed as dots and Mg atoms as bubbles); (b) selected part orientated to display (3 1 1)Al atomic planes on the right of the planar segregation; (c) 2-D chemical map showing the Mg concentration fluctuations within the volume; (d) concentration profile computed across the segregation (sampling volume thickness 1 nm).

precipitation of that phase. It should also be noted that Mg is not homogeneously distributed along the boundary; some significant local composition fluctuations do exist. Furthermore, no other elements were detected along the grain boundary.

SPD-induced grain boundary segregations in Al alloys have already been experimentally observed, e.g. in UFG 6061 alloy processed by HPT [14] and in 7136 alloy processed by equal-channel angular pressing [15]. However, in these specific cases the concentration of solute elements, Mg in particular, did not exceed a few atomic per cent. It is natural to suppose that significantly elevated Mg content revealed in the present study could influence the mechanical behaviour of the investigated alloy. The influence should be significant, since both XRD and APT measurements testified that the Mg concentration in solid solution of UFG 1570 alloy was significantly decreased, so one could expect a certain softening of the UFG 1570 alloy instead of the observed strengthening.

It is well established that deformation of UFG materials (with grains larger than 30–50 nm) is mainly associated with intragranular movement of lattice dislocations [3,5]. In addition, dislocations are generated at grain boundaries and move through a grain to be captured by an opposite grain boundary. In this case the rate-controlling mechanism is "dislocation-grain boundary" interaction. Elevated concentration of solutes in grain boundaries can suppress emission of dislocations from such boundaries due to solute drag. Moreover, nonuniform distribution of solutes along a grain boundary would pin a dislocation, resulting in it being emitted discontinuously – different regions of a segregation with various Mg content will drag corresponding regions of a dislocation differently, breaking it into segments at the given stress. Thus, the characteristic length, and, correspondingly, activation volume of the deformation process will be reduced.

In Ref. [16] the authors observed a somewhat similar effect of sulfur segregation in cold-worked Zr–1 Nb alloy. They showed that even a small amount of sulfur segregated at grain boundaries leads to a noticeable decrease in V_a (from 110 to $80b^3$ at room temperature) and additional strengthening of the alloy. They also explained the phenomena by suggesting that sulfur atoms pin dislocation segments, preventing these from being emitted from a GB.

Let us consider the effect of reducing the activation volume in a more detailed way. The stress required for a dislocation motion can be calculated by the model of an individual dislocation emission from a grain boundary [17]. According to the model, the flow stress is defined by the size of the dislocation source or the activation volume, both of which depend on the material structure.

The critical stress for the emission of an individual dislocation may be expressed as [17]:

$$\sigma = \alpha \frac{Gb}{L}\left[\ln\frac{L}{b} - 1.65\right], \tag{1}$$

where σ is yield stress, G is the shear modulus, b is the Burgers vector, L is the length of the dislocation or its source, and α is a constant.

When deformation is realized by dislocation motion, L can be expressed in terms of activation volume v:

$$L = \frac{v}{b^2}, \tag{2}$$

which is accordingly related to the strain-rate sensitivity m [17]:

$$m = \frac{\sqrt{3}kT}{\sigma v}. \tag{3}$$

Based on these relations, the strain-rate sensitivity can be estimated, suggesting that the increase in strength of the 1570 alloy in UFG condition is achieved due to the change in chemical composition in the grain boundary regions with corresponding change in the activation volume v/b^3 (or dislocation source length L/b). In order to fit the reported strength of the UFG 1570 alloy using Eq. (2), the activation volume value should lie within the range of $v \sim 12 - 17b^3$, which corresponds to $m \sim 0.02$ according to Eq. (3). This strain-rate sensitivity value is similar to the experimentally measured m for the UFG Al alloys at ambient temperature [18], which is in agreement with the estimations of V_a given above. However, to fully clarify this point, further measurements of the strain-rate sensitivity of the present UFG alloy will shortly be carried out.

[1] E.O. Hall, Proc. Phys. Soc. Lond. 64B (1951) 747–753.
[2] N.J. Petch, J. Iron Steel Inst. 174 (1953) 25–28.
[3] C. Pande, K. Cooper, Prog. Mater. Sci. 54 (2009) 689–706.
[4] F. Louchet, J. Weiss, T. Richeton, Phys. Rev. Lett. 97 (1–4) (2006) 75504.
[5] R.Z. Valiev, R.K. Islamgaliev, I.V. Alexandrov, Prog. Mater. Sci 45 (2000) 103–189.
[6] M. Murashkin, A. Kilmametov, R. Valiev, Phys. Met. Metall. 106 (2008) 90–96.
[7] H.P. Klug, L.E. Alexander, X-ray Diffraction Procedures for Polycrystalline and Amorphous Materials, John Wiley & Sons, New York, 1974.
[8] G.D. Costa, F. Vurpillot, A. Bostel, M. Bouet, B. Deconihout, Rev. Sci. Instrum. 76 (2005) 013304.
[9] Z. Horita, D.J. Smith, M. Furukawa, M. Nemoto, R.Z. Valiev, T.G. Langdon, J. Mater. Res. 11 (1996) 1880–1890.
[10] N. Tsuji, in: Y.T. Zhu, V. Varyukhin (Eds.), Nanostructured Materials by High-pressure Severe Plastic Deformation, Springer Netherlands, 2006, pp. 227–234.
[11] M. Furukawa, Z. Horita, M. Nemoto, R.Z. Valiev, T.G. Langdon, Philos. Mag. A 78 (1998) 203–215.
[12] M. Markushev, M. Murashkin, Mater. Sci. Eng. A 367 (2004) 234–242.
[13] J.E. Hatch (Ed.), Aluminum: Properties and Physical Metallurgy, ASM International, 1984.
[14] G. Nurislamova, X. Sauvage, M. Murashkin, R. Islamgaliev, R. Valiev, Philos. Mag. Lett. 88 (2008) 459–466.
[15] G. Sha, S.P. Ringer, Z.C. Duan, T.G. Langdon, Int. J. Mater. Res. (2009) 1674–1678.
[16] K. Chang, S. Hong, J. Nucl. Mater. 373 (2008) 16–21.
[17] J. Lian, C. Gu, Q. Jiang, Z. Jiang, J. Appl. Phys. 99 (2006) 076103.
[18] R. Hayes, D. Witkin, F. Zhou, E. Lavernia, Acta Mater. 52 (2004) 4259–4271.